Heterodisulfide reductase from *Methanothermobacter marburgensis* contains an active-site [4Fe–4S] cluster that is directly involved in mediating heterodisulfide reduction

Evert C. Duin[a,*], Shahla Madadi-Kahkesh[a], Reiner Hedderich[a], Michael D. Clay[b], Michael K. Johnson[b]

[a] *Max-Planck-Institut für terrestrische Mikrobiologie and Laboratorium für Mikrobiologie, Fachbereich Biologie, Philipps-Universität, Karl-von-Frisch-Strasse, D-35043 Marburg, Germany*
[b] *Department of Chemistry and Center for Metalloenzyme Studies, University of Georgia, Athens, GA 30602, USA*

Received 9 November 2001; revised 3 January 2002; accepted 3 January 2002

First published online 22 January 2002

Edited by Hans Eklund

Abstract Heterodisulfide reductases (HDRs) from methanogenic archaea are iron–sulfur flavoproteins or hemoproteins that catalyze the reversible reduction of the heterodisulfide (CoM-S–S-CoB) of the methanogenic thiol coenzymes, coenzyme M (CoM-SH) and coenzyme B (CoB-SH). In this work, the ground- and excited-state electronic properties of the paramagnetic Fe–S clusters in *Methanothermobacter marburgensis* HDR have been characterized using the combination of electron paramagnetic resonance and variable-temperature magnetic circular dichroism spectroscopies. The results confirm multiple $S = 1/2$ $[4Fe–4S]^{+}$ clusters in dithionite-reduced HDR and reveal spectroscopically distinct $S = 1/2$ $[4Fe–4S]^{3+}$ clusters in oxidized HDR samples treated separately with the CoM-SH and CoB-SH cosubstrates. The active site of HDR is therefore shown to contain a [4Fe–4S] cluster that is directly involved in mediating heterodisulfide reduction. The catalytic mechanism of HDR is discussed in light of the crystallographic and spectroscopic studies of the related chloroplast ferredoxin:thioredoxin reductase class of disulfide reductases. © 2002 Published by Elsevier Science B.V. on behalf of the Federation of European Biochemical Societies.

Key words: Heterodisulfide reductase; Iron–sulfur protein; Magnetic circular dichroism; Ferredoxin:thioredoxin reductase; *Methanothermobacter marburgensis*

1. Introduction

In the final steps of methanogenesis in methanogenic archaea, the central intermediate methyl coenzyme M (CH_3-S-CoM) reacts with coenzyme B (CoB-SH) to form methane and the heterodisulfide CoM-S–S-CoB. This process is catalyzed by methyl coenzyme M reductase [1]. The heterodisulfide functions as the terminal electron acceptor of an energy-conserving electron transport chain, a process called disulfide respiration [2,3]. Heterodisulfide reductase (HDR) is the key enzyme of this process, catalyzing the reversible reduction of CoM-S–S-CoB to the thiol coenzymes, coenzyme M (CoM-SH) and CoB-SH. HDR exhibits a high specificity for the substrates of the reduction (CoM-S–S-CoB) and oxidation (CoM-SH plus CoB-SH) reactions [4].

HDR from *Methanothermobacter marburgensis* is composed of three subunits, HdrA, HdrB and HdrC. HdrA contains a typical FAD binding motif and four binding motifs for $[4Fe–4S]^{2+,+}$ clusters. HdrC contains two additional binding motifs for $[4Fe–4S]^{2+,+}$ clusters while HdrB contains no characteristic binding motif of known cofactors [5]. However, it contains the sequence motif **C**-x_n-**CC**-x_n-**C**-xx-**C**-x_n-**C**-x_n-**CC**-x_n-**C**-xx-**C**, which is conserved in HDR from *Methanosarcina barkeri* (contains only two binding motifs for $[4Fe–4S]^{2+,+}$ clusters in addition to two *b*-type cytochromes) and in the thiol:fumarate reductase from *M. marburgensis*. The latter enzyme catalyzes the reduction of fumarate to succinate using reducing equivalents derived from the oxidation of CoM-SH and CoB-SH to form the heterodisulfide [6]. It has been proposed that some of these cysteine residues might coordinate an additional iron–sulfur cluster [6,7] and that the mechanism of disulfide reduction is closely related to that of the ferredoxin:thioredoxin reductase (FTR) from chloroplasts and cyanobacteria.

FTR catalyzes the reduction of a disulfide on the substrate, thioredoxin, in two one-electron steps, using reduced [2Fe–2S] ferredoxin as the electron donor. The enzyme contains a $[4Fe–4S]^{2+}$ cluster as the sole prosthetic group in addition to an active-site disulfide [8]. A mechanistic scheme has been proposed for FTR involving two sequential one-electron transfers from ferredoxin. The role of the $[4Fe–4S]^{2+}$ cluster is both to mediate electron transfer to the active-site disulfide and to stabilize the formal cysteinyl radical that results from initial one-electron reduction of the active-site disulfide, via reduction and coordination of one of the active-site cysteines to an undefined site on the resultant oxidized $[4Fe–4S]^{3+}$ cluster. This model is based on extensive spectroscopic studies of *N*-ethylmaleimide-modified FTR (NEM-FTR) from spinach in which one of the disulfide cysteines is alkylated [9,10]. Under turnover conditions, FTR shows the same EPR signal as observed for the $[4Fe–4S]^{3+}$ cluster in NEM-FTR, indicat-

*Corresponding author. Fax: (49)-6421-178299.
E-mail address: duin@mailer.uni-marburg.de (E.C. Duin).

Abbreviations: HDR, heterodisulfide reductase; CoM-SH, coenzyme M or 2-mercaptoethane sulfonate; CoB-SH, coenzyme B or 7-mercaptoheptanoylthreonine phosphate; CoM-S–S-CoB, heterodisulfide of CoM-SH and CoB-SH; CoM-HDR, oxidized HDR incubated with CoM-SH; CoB-HDR, oxidized HDR incubated with CoB-SH; FTR, ferredoxin:thioredoxin reductase; NEM-FTR, *N*-ethylmaleimide-modified FTR; VTMCD, variable-temperature magnetic circular dichroism; DTT, dithiothreitol

0014-5793/02/$22.00 © 2002 Published by Elsevier Science B.V. on behalf of the Federation of European Biochemical Societies.
PII: S0014-5793(02)02281-0

ing that the latter species is a stable analog of a one-electron-reduced enzymatic intermediate. Recently the crystal structure of FTR from *Synechocystis* sp. PCC6803 was solved. The structure shows a cysteine disulfide asymmetrically positioned relative to the cluster with one of the S atoms at a distance of 3.1 Å from both a cluster Fe and the S atom of a cluster-ligating cysteinate, and 3.5 Å from a cluster μ_3-S atom. The structure, therefore, reinforces the proposal that the one-electron-reduced intermediate is stabilized by attachment of the proximal cysteine of the cleaved active-site disulfide to the cluster, and suggests that a cluster Fe is the most likely point of attachment to yield an intermediate involving a [4Fe–4S] cluster with a five-coordinate Fe site [11].

The number, type and redox properties of Fe–S clusters in *M. marburgensis* HDR has been investigated by electron paramagnetic resonance (EPR) and resonance Raman spectroscopies [12]. Oxidized HDR samples exhibited no signals attributable to paramagnetic Fe–S clusters and the resonance Raman spectrum was readily interpreted exclusively in terms of $S = 0$ $[4Fe–4S]^{2+}$ clusters. In the absence of substrates, dye-mediated EPR redox titrations revealed a high-potential $[4Fe–4S]^{2+,+}$ center ($E_m = -153$ mV versus NHE at pH 7.6, $S = 1/2$ $[4Fe–4S]^{+}$ cluster with $g = 2.058$, 1.938 and 1.863) and multiple low-potential $[4Fe–4S]^{2+,+}$ centers ($E_m < -300$ mV versus NHE at pH 7.6, magnetically interacting $S = 1/2$ $[4Fe–4S]^{+}$ clusters exhibiting a complex spectrum with apparent g values of 2.052, 1.933 and 1.887 and broad wings). Similar results were obtained for redox titrations on HDR from *Methanosarcina thermophila* [13], with the two $[4Fe–4S]^{2+,+}$ clusters having midpoint potentials of −100 mV and −400 mV.

EPR signals of potential relevance to the catalytic cycle were observed on reaction of oxidized HDR with either CoM-SH or CoB-SH, the cosubstrates for the oxidative reaction [12]. In the presence of CoM-SH, a novel $S = 1/2$ resonance was observed at temperatures below 50 K, with principal g values of 2.013, 1.991 and 1.938. The resonance is lost on reduction ($E_m = -185$ mV versus NHE at pH 7.6) and on reaction with CoB-SH. Hence, it was attributed to the product of the oxidative half-reaction that occurs in the absence of CoB-SH, in which case it is likely to correspond to a trapped intermediate in the catalytic cycle. A species with similar g values, $g = 2.018$, 1.996 and 1.954, and relaxation properties was observed when oxidized HDR was treated with CoB-SH. However, redox titrations revealed a significantly higher midpoint potential ($E_m = -30$ mV versus NHE at pH 7.6) than the CoM-SH-generated species and argue against a role as an intermediate in the HDR catalytic cycle.

The CoM-SH-induced EPR signal in *M. marburgensis* HDR showed ^{57}Fe broadening [12], indicating it corresponds to a paramagnetic Fe–S center rather than an organic radical. However, the nature of the Fe–S cluster responsible for this EPR signal has still to be determined, since the g value anisotropy and relaxation is distinct from any known type of oxidized Fe–S cluster. In an attempt to characterize the type and oxidation state of the paramagnetic Fe–S centers in oxidized and reduced derivatives of *M. marburgensis* HDR, we report here on the results of parallel variable-temperature magnetic circular dichroism (VTMCD) and EPR studies. The results strengthen the link between the mechanisms of HDR and FTR and suggest that both function via one-electron-reduced intermediates involving an active-site $[4Fe–4S]^{3+}$ cluster coordinated by five thiolate ligands.

2. Materials and methods

2.1. Materials

M. marburgensis (formerly *Methanobacterium thermoautotrophicum*, strain Marburg) is the strain deposited under DSM 2133 in the Deutsche Sammlung von Mikroorganismen und Zellkulturen (Braunschweig). Coenzyme B ((+)-(2*S*,3*R*)-*N*-[7-mercaptoheptanoyl]-*O*-phospho-threonine) was synthesized via the symmetric disulfide CoB-S–S-CoB by reduction with $NaBH_4$ [14,15]. Coenzyme M (2-mercaptoethane sulfonate) was obtained from Merck. Duroquinone was obtained from Sigma.

2.2. Sample preparation and handling

M. marburgensis was cultured in a 10 l fermenter at 65°C on 80% H_2/20% CO_2/0.1% H_2S as previously described [16]. Cells were harvested under exclusion of oxygen and stored at −80°C. HDR was purified under strictly anaerobic conditions under an atmosphere of N_2/H_2 (95%/5%) at room temperature using the published protocol [12]. All buffers contained 2 mM dithiothreitol (DTT). Proteins were judged to be >95% pure by SDS–PAGE. The protein concentration was determined by using the method of Bradford [17] with bovine serum albumin (Serva) as standard. The method was calibrated by a quantitative amino acid analysis. Prior to spectroscopic measurements of *M. marburgensis* HDR, DTT was removed by ultrafiltration.

For spectroscopic measurements, the enzyme was concentrated to 400 μM by centrifugation using a Centricon with a 100 kDa cut off (Millipore). For every sample 100 μl was taken, which was diluted to 220 μl by adding buffer and/or the solutions of the respective reagents. Additionally 280 μl of ethylene glycol was added to all the samples as glassing agent. The 500 μl sample was then split in two to make parallel EPR and MCD samples. For the reduced sample, HDR was reduced by anaerobic addition of 10 mM dithionite. The CoM-HDR and CoB-HDR samples were made by oxidizing the protein with 0.5 mM duroquinone ($E^{\circ\prime} = +86$ mV vs. NHE) followed by addition of 10 mM CoM-SH or 10 mM CoB-SH, and incubation at room temperature for 5 min. The sample of NEM-FTR from *Synechocystis* sp. PCC6803 was a gift from Dr. Peter Schürmann (Université de Neuchâtel, Switzerland).

2.3. Spectroscopic measurements

VTMCD spectroscopic measurements were performed using an Oxford Instruments Spectromag 4000 split-coil superconducting magnet mated to a Jasco J715 spectropolarimeter. The experimental protocols used in VTMCD studies for accurate sample temperature and magnetic field measurements, anaerobic sample handling, and assessment of residual strain in frozen samples have been described elsewhere [18,19]. The MCD intensities are expressed as $\Delta\varepsilon$ ($\varepsilon_{LCP} - \varepsilon_{RCP}$) where ε_{LCP} and ε_{RCP} are the molar extinction coefficients for the absorption of left and right circularly polarized light, respectively.

EPR spectra at X-band (9 GHz) were obtained with a Bruker EMX spectrometer or Bruker ESP 300E spectrometer fitted with Oxford Instruments ESR 900 flow cryostats and ITC4 temperature controllers. Spin quantitations were carried out under non-saturating conditions using 10 mM copper perchlorate as the standard (10 mM $CuSO_4$; 2 M $NaClO_4$; 10 mM HCl).

3. Results

Fig. 1 shows a comparison of the VTMCD spectra and parallel EPR spectra for the dithionite-reduced, oxidized CoM-SH and oxidized CoB-SH derivatives of *M. marburgensis* HDR, and oxidized NEM-FTR from *Synechocystis* sp. PCC6803. Only paramagnetic metal chromophores exhibit intense VTMCD bands and this enables characterization of the ground- and excited-state properties of paramagnetic Fe–S centers in HDR samples in which the absorption spectrum is dominated by contributions from diamagnetic Fe–S clusters and FAD. Dithionite-reduced HDR exhibits VTMCD spectra characteristic of multiple $S = 1/2$ $[4Fe–4S]^{+}$ clusters [20–22] (Fig. 1A, left panel). The EPR signal comprises an intense radical signal from an anionic (red) flavin semiquinone cen-

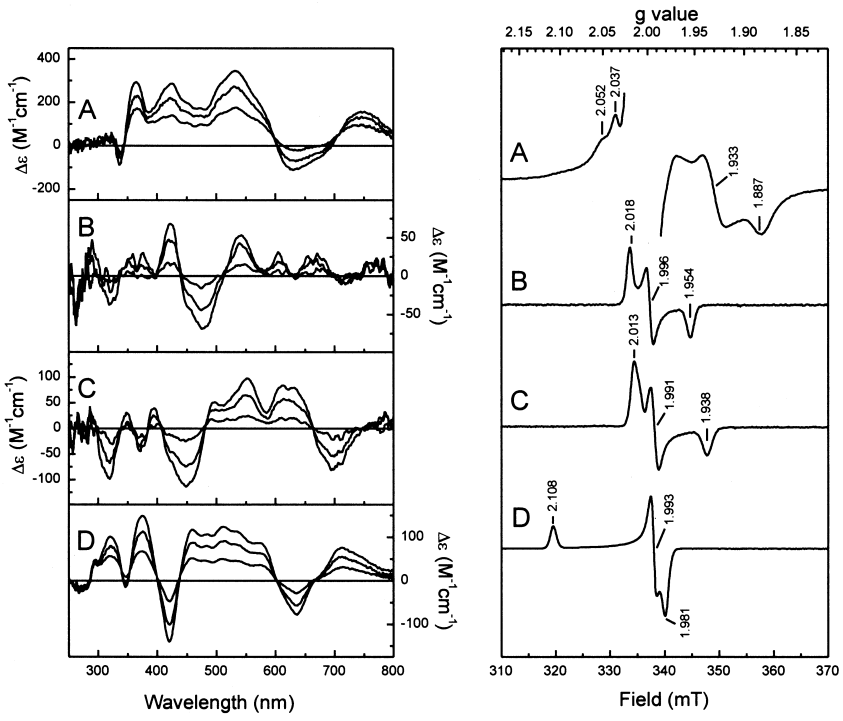

Fig. 1. Comparison of the VTMCD and EPR spectra of different forms of HDR from *M. marburgensis*, and NEM-FTR from *Synechocystis* sp. PCC6803. Left panel: VTMCD spectra recorded at 1.7, 4.2 and 10 K with an applied magnetic field of 6 T. All transitions increase in intensity with decreasing temperature. Right panel: EPR spectra recorded at 5 K (A) and 30 K (B–D) with 2 mW microwave power and 0.6 mT modulation amplitude at a microwave frequency of 9.43 GHz. A: Dithionite-reduced HDR; B: CoB-HDR, duroquinone-oxidized HDR incubated with CoB-SH; C: CoM-HDR, duroquinone-oxidized HDR incubated with CoM-SH; D: oxidized NEM-FTR.

tered at $g = 2$ and an Fe–S cluster resonance with inflections at $g = 2.05$, 2.04, 1.93 and 1.89 with broad wings extending to high and low field (Fig. 1A, right panel) [12]. The complex Fe–S cluster resonance has been attributed to weak intercluster spin–spin interactions between multiple $S = 1/2$ $[4Fe–4S]^{+}$ clusters [12] and accounts for 3–4 spins/molecule after subtraction of the contribution from the flavin radical species. Variable-temperature, variable-field MCD saturation magnetization studies [23,24] indicate that all transitions arise from $S = 1/2$ ground states (data not shown) and the intensity of the VTMCD spectrum is consistent with 3–4 $S = 1/2$ $[4Fe–4S]^{+}$ clusters. Primary sequence considerations predict six $[4Fe–4S]^{2+,+}$ clusters in *M. marburgensis* HDR. Consequently the EPR and VTMCD results suggest that two or three $[4Fe–4S]^{2+,+}$ clusters are not reduced by dithionite or that multiple $[4Fe–4S]^{2+,+}$ clusters are only partially reduced by dithionite.

Oxidation of HDR using duroquinone followed by addition of CoM-SH to give CoM-HDR or CoB-SH to give CoB-HDR results in similar $S = 1/2$ EPR signals that are readily observed under non-saturating conditions at 30 K: $g = 2.013$, 1.991, 1,938, accounting for 1.0 ± 0.1 spin/molecule for CoM-HDR (Fig. 1C, right panel); $g = 2.018$, 1.996, 1.954, accounting for 0.5 ± 0.1 spin/molecule for CoB-HDR (Fig. 1B, right panel). No additional EPR signals were detected at lower temperatures for either CoM-HDR or CoB-HDR indicating that all the $[4Fe–4S]^{2+,+}$ clusters are oxidized and therefore diamagnetic. Hence the VTMCD spectra of CoM-HDR (Fig. 1C, left panel) and CoB-HDR (Fig. 1B, left panel) are expected to facilitate selective characterization of the electronic transitions associated Fe–S center responsible for these novel EPR signals. This is confirmed by variable-temperature, variable-field MCD saturation magnetization studies [23,24], which indicate that each of the temperature-dependent MCD bands of CoM-HDR and CoB-HDR originates exclusively from the $S = 1/2$ ground state responsible for the EPR signals (data not shown). The VTMCD spectra of both CoB-HDR and CoM-HDR are different from each other (cf. Fig. 1B,C, left panel) and both are distinct from those associated with the most common types of oxidized paramagnetic Fe–S clusters, i.e. cubane and linear $[3Fe–4S]^{+}$ clusters [25] and HiPIP-type $[4Fe–4S]^{3+}$ clusters [20,26]. However, the VTMCD spectra of CoM-HDR and CoB-HDR both show correspondence to that observed for the novel type of $[4Fe–4S]^{3+}$ cluster found in NEM-FTR [9,10] (Fig. 1D, left panel). The similarity is particularly striking when comparing the VTMCD spectra of CoM-HDR and NEM-FTR. Both have the same pattern of positive and negative bands with equivalent bands shifted to lower energy by ~ 2000 cm^{-1} in CoM-HDR. The correspondence is less immediately apparent between the VTMCD spectra of CoB-HDR and NEM-FTR due to changes in the relative intensities of the MCD bands and a further red shift of each of the bands. Nevertheless the pattern of VTMCD bands observed in NEM-FTR is clearly preserved in both CoM-HDR and CoB-HDR indicating each contains a similar type of novel $[4Fe–4S]^{3+}$ cluster.

The close correspondence of CoM-HDR and CoB-HDR with NEM-FTR in terms of excited state properties is not so apparent in terms of the ground-state properties. Although all three clusters exhibit $S = 1/2$ ground states, NEM-FTR exhibits a near-axial g tensor with $g_{\parallel} = 2.11 > g_{\perp} = 1.99$ ($g_{av} = 2.03$), while CoM-HDR and CoB-HDR both exhibit approximately axial g tensors with $g_{\parallel} = 1.94 < g_{\perp} = 2.00$

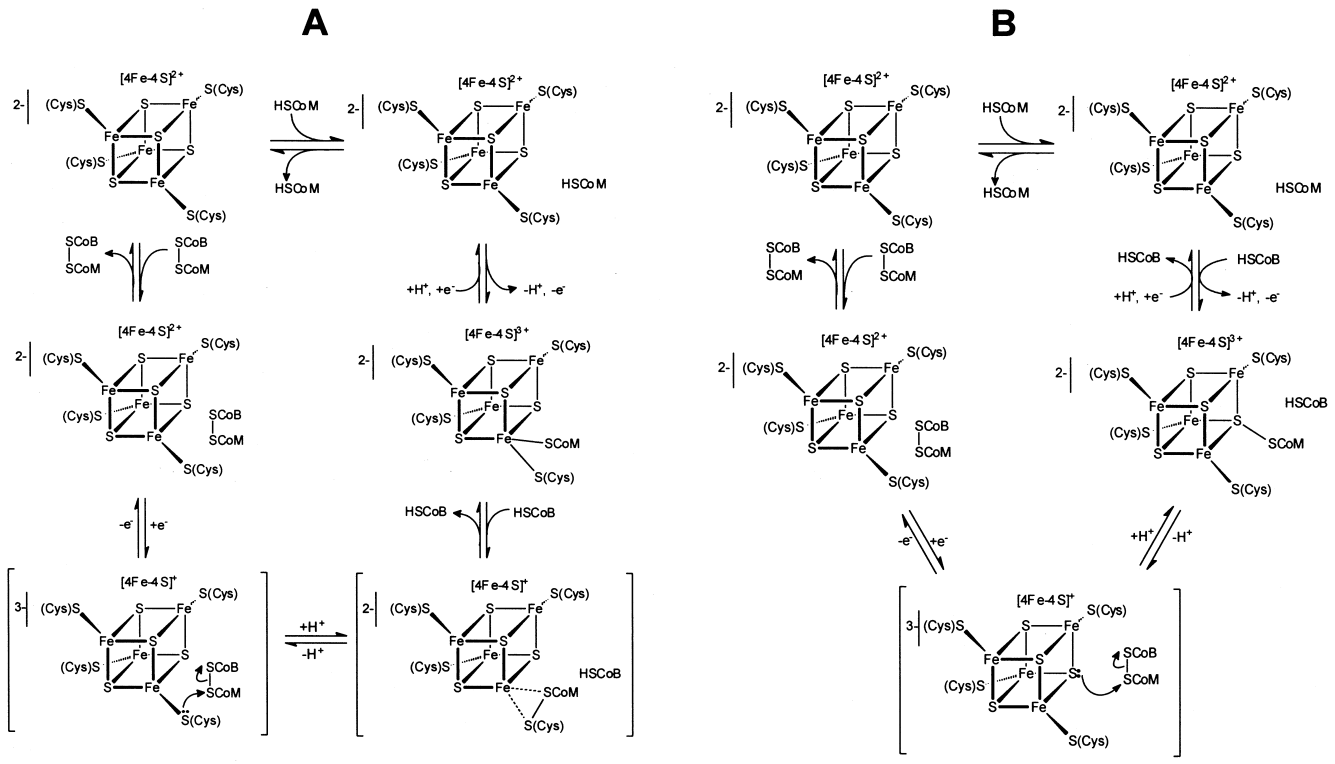

Fig. 2. Proposed active-site mechanisms for the reversible heterodisulfide/dithiol reaction catalyzed by HDR. The oxidation state of the [4Fe–4S] cores is indicated above each of the cubane clusters and the charge of the cluster including the thiolate ligands is indicated to the left of the lines next to the clusters. Transient intermediates are shown in parentheses and the electron arrows on one of the transient intermediates correspond to the reductase reaction.

($g_{av} = 1.98$) and $g_{\parallel} = 1.95 < g_{\perp} = 2.01$ ($g_{av} = 1.99$), respectively (cf. Fig. 1B–D, right panel). Moreover, the relaxation properties of EPR signals are also very different. The NEM-FTR resonance can be observed without broadening up to 150 K, while the CoM-HDR and CoB-HDR resonances are too broad to observe above 60 K.

4. Discussion

The nature of the active-site Fe–S cluster of *M. marburgensis* HDR is difficult to assess due to the presence of six conventional $[4Fe–4S]^{2+,+}$ clusters in addition to FAD. Since HdrB is presumed to contain the active-site cluster, whereas the conventional $[4Fe–4S]^{2+,+}$ clusters and FAD are located on HdrA or HdrC, our initial attempts to address this question involved overexpressing the *hdrB* gene in *Bacillus subtilis* and characterizing the purified HrdB gene product [12]. The overexpression yielded a protein that contained a $[2Fe–2S]^{2+}$ cluster as assessed by absorption and resonance Raman spectroscopy [12]. However, the recombinant HdrB protein did not show activity in assays with CoM-SH and CoB-SH or heterodisulfide and there is no spectroscopic evidence for a $[2Fe–2S]^{2+}$ cluster in holo-HDR [12]. Hence it seems likely that the $[2Fe–2S]^{2+}$ cluster is an artifact of heterologous expression of this subunit in isolation.

The VTMCD studies of CoB-HDR and CoM-HDR presented herein provide compelling evidence for the presence of a novel type of $[4Fe–4S]^{3+}$ cluster at the active site of HDR with electronic and redox properties similar to those of the anomalous $[4Fe–4S]^{3+}$ cluster previously characterized in NEM-FTR [9,10]. The assignment of the $S = 1/2$ center in NEM-FTR to a $[4Fe–4S]^{3+}$ cluster is based on detailed spectroscopic characterization using the combination of UV-visible absorption, VTMCD, resonance Raman, and ENDOR [10]. Furthermore, the novel electronic and redox properties of the $[4Fe–4S]^{3+}$ cluster in NEM-FTR compared to conventional HiPIP-type $[4Fe–4S]^{3+}$ clusters, i.e. different excited-state electronic properties as assessed by VTMCD and a 600 mV decrease in midpoint potential, have been attributed to ligation of a fifth cysteinate to either a cluster μ_3-S or Fe atom [10]. On the basis of the crystal structure of *Synechocystis* FTR [11] and the 600 mV decrease in midpoint potential for synthetic $[4Fe–4S]^{3+,2+}$ clusters that accompanies the change from monodentate to bidentate thiolate ligation at a specific Fe site [27], coordination of the additional thiolate to Fe to give a five-coordinate Fe site would appear to be the most likely point of attachment. However, as discussed below, it is not possible to rule out the alternative mode of attachment involving covalent linkage of the additional thiolate to a cluster μ_3-S. Under both scenarios, the parallel trends in the redox potentials and energies of the electronic transitions of the $[4Fe–4S]^{3+}$ clusters in CoB-HDR ($E_m = -30$ mV [12]), CoM-HDR ($E_m = -185$ mV [12]), and NEM-FTR ($E_m = -210$ mV [8]) are best interpreted in terms of differences in the additional ligated thiolate ligand, i.e. CoB-S^-, CoM-S^-, and (Cys)S^-, respectively.

Understanding the origin of the marked differences in ground-state *g*-value anisotropy and relaxation properties of the $[4Fe–4S]^{3+}$ clusters in CoM-HDR, CoB-HDR, NEM-FTR and HiPIPs is a fascinating problem that will require detailed ^{57}Fe ENDOR and Mössbauer studies. In conventional HiPIP-type $[4Fe–4S]^{3+}$ clusters, the $S = 1/2$ ground state

($g = 2.12$–2.15, 2.03–2.04, 2.02–2.03 and observable < 30 K) has been rationalized in terms of antiferromagnetic interaction between a $S = 3$ or 4 diferric pair and a $S = 9/2$ or 7/2 mixed-valence ferric/ferrous pair [28–30]. Addition of an additional thiolate ligand at a specific Fe site would favor a valence-localized ferric site and thereby changes in the intracluster magnetic interactions and valence delocalization. Likewise modification of one μ_3-S^{2-} by covalent attachment of a thiolate would be expected to result in changes in intracluster magnetic interactions and valence delocalization. In both cases, such changes would be expected to be manifest in terms of differences in the ground-state spin or g-value anisotropy and differences in relaxation properties resulting from changes in the energies of low-lying excited states. More detailed spectroscopic studies of NEM-FTR, CoM-HDR, and CoB-HDR are required to address the origin of the differences in ground-state properties and thereby the site of attachment of the fifth thiolate ligand.

Finally, we turn to the implications of the results presented herein for the mechanism of HDR. Several lines of evidence argue in favor of a mechanism involving direct interaction of the heterodisulfide substrate with the active-site [4Fe–4S] cluster rather than the FTR-type mechanism in which cleavage of the substrate disulfide by the [4Fe–4S] cluster is mediated by an active-site disulfide in close proximity to the cluster [11]. First, the marked differences in the redox and electronic excited state properties of the $[4Fe–4S]^{3+}$ clusters in CoB-HDR and CoM-HDR argue for direct attachment to the cluster, as discussed above. Second, the $[4Fe–4S]^{3+}$ species in HDR are readily formed under oxidizing conditions on addition of exogenous thiols such as CoM-SH, CoB-SH, DTT or β-mercaptoethanol [12]. This does not occur in FTR since the active-site disulfide that is present in oxidized samples can only be cleaved under reducing conditions using the physiological electron donor, reduced ferredoxin, or mediator dyes such as reduced viologens [31]. The $[4Fe–4S]^{3+}$ species in FTR is only observed as a stable species on oxidation when one of the active-site cysteine residues has been alkylated, and therefore not available to reform the active-site disulfide on oxidation, leaving the free cysteine available to interact with the cluster. Third, *M. marburgensis* HDR is not inhibited by cysteine alkylating reagents at concentrations up to 2 mM [12], whereas cysteine alkylating reagents are potent inhibitors of FTR as a result of alkylation of the interchange thiol of the active-site disulfide [32].

The above considerations lead us to propose alternative mechanistic schemes for the reversible heterodisulfide/dithiol cleavage reaction that is catalyzed by HDR in two one-electron steps (see Fig. 2). It is not known if the active-site $[4Fe–4S]^{2+}$ cluster is reducible to a stable $[4Fe–4S]^{+}$ state in the absence of substrate, CoB-S–S-CoM. By analogy with FTR [9,10], it is proposed that the initial one-electron reduction of the $[4Fe–4S]^{2+}$ cluster in the resting enzyme only occurs in the presence of substrate. The $[4Fe–4S]^{+}$ cluster is therefore depicted as a transient intermediate that immediately reacts to cleave the heterodisulfide. Since disulfides are generally cleaved via nucleophilic substitution reactions, it is proposed that either a cluster ligating cysteinate (scheme A in Fig. 2) or a cluster μ_3-S^{2-} (scheme B in Fig. 2) becomes sufficiently electron-rich on reduction to initiate the nucleophilic attack on CoM-S–S-CoB. The former is more attractive in terms of crystal structure of FTR, since the S of the proximal cysteine of the active-site disulfide is 3.1 Å from the S of a coordinating cysteine and 3.5 Å from a cluster μ_3-S [11]. However, the latter is more consistent with S K-edge X-ray absorption studies of biological and synthetic $[4Fe–4S]^{2+}$ centers which indicate greater electron density on the S atoms of μ_3-bridging sulfides than those of coordinated thiolates [33–35]. In scheme A, nucleophilic attack results in the formation of CoB-SH and a transient intermediate involving a weakly coordinated CoM-S–S-Cys heterodisulfide which is then cleaved by accepting two electrons from the cluster to give a $[4Fe–4S]^{3+}$ cluster with one Fe bound by both Cys-S^{-} and CoM-S^{-} thiolates. In scheme B, nucleophilic attack results in the formation of CoB-SH and a $[4Fe–4S]^{3+}$ cluster with CoM-S^{-} attached to a cluster μ_3-S. In both schemes, a second one-electron reduction then reduces the novel $[4Fe–4S]^{3+}$ cluster back to the $[4Fe–4S]^{2+}$ resting state, with concomitant dissociation and protonation of CoM-S^{-}. The evidence that CoM-S^{-} rather than CoB-S^{-} binds to the cluster is based on the observation that the CoM-HDR EPR signal is lost on addition of CoB-SH and that the redox potential for CoM-HDR is close to the heterodisulfide/dithiol couple.

These mechanistic schemes provide the basis for future experiments to address the catalytic cycle of HDR. EPR and ENDOR experiments using CoM-^{33}SH and CoM-SeH are planned to evaluate the proposal that the heterodisulfide/dithiol substrates react directly with the cluster in HDR. These experiments, coupled with Mössbauer and Se-EXAFS (using CoM-SeH) will then be used to address the site of cluster attachment of CoM, in the absence of more direct structural evidence from X-ray crystallography.

Acknowledgements: This work was supported by the Max-Planck-Gesellschaft, by the Deutsche Forschungsgemeinschaft, by the Fonds der Chemischen Industrie, by the National Institutes of Health (GM62524 to M.K.J.), and by a fellowship from the Humboldt Stiftung to E.D. We thank Dr. Peter Schürmann for supplying the sample of *Synechocystis* NEM-FTR for comparative spectroscopic studies.

References

[1] Thauer, R.K. (1998) Microbiology 144, 2377–2406.
[2] Deppenmeier, U., Lienard, T. and Gottschalk, G. (1999) FEBS Lett. 457, 291–297.
[3] Hedderich, R., Klimmek, O., Kröger, A., Dirmeier, R., Keller, M. and Stetter, K.O. (1998) FEMS Microbiol. Rev. 22, 353–381.
[4] Hedderich, R., Berkessel, A. and Thauer, R.K. (1989) FEBS Lett. 255, 67–71.
[5] Hedderich, R., Koch, J., Linder, D. and Thauer, R.K. (1994) Eur. J. Biochem. 225, 253–261.
[6] Heim, S., Künkel, A., Thauer, R.K. and Hedderich, R. (1998) Eur. J. Biochem. 253, 292–299.
[7] Künkel, A., Vaupel, M., Heim, S., Thauer, R.K. and Hedderich, R. (1997) Eur. J. Biochem. 244, 226–234.
[8] Droux, M., Jacquot, J.-P., Miginac-Maslow, M., Gadal, P., Huet, J.C., Crawford, N.A., Yee, B.C. and Buchanan, B.B. (1987) Arch. Biochem. Biophys. 252, 426–439.
[9] Staples, C.R., Ameyibor, E., Fu, W., Gardet-Salvi, L., Stritt-Etter, A.-L., Schürmann, P., Knaff, D.B. and Johnson, M.K. (1996) Biochemistry 35, 11425–11434.
[10] Staples, C.R., Gaymard, E., Stritt-Etter, A.-L., Telser, J., Hoffman, B.M., Schürmann, P., Knaff, D.B. and Johnson, M.K. (1998) Biochemistry 37, 4612–4620.
[11] Dai, S., Schwendtmayer, C., Schürmann, P., Ramaswamy, S. and Eklund, H. (2000) Science 287, 655–658.
[12] Madadi-Kahkesh, S., Duin, E.C., Heim, S., Albracht, S.P.J., Johnson, M.K. and Hedderich, R. (2001) Eur. J. Biochem. 268, 2566–2577.

[13] Simianu, M., Murakami, E., Brewer, J.M. and Ragsdale, S.W. (1998) Biochemistry 37, 10027–10039.
[14] Kobelt, A., Pfaltz, A., Ankel-Fuchs, D. and Thauer, R.K. (1987) FEBS Lett. 214, 265–268.
[15] Ellermann, J., Hedderich, R., Böcher, R. and Thauer, R.K. (1988) Eur. J. Biochem. 172, 669–677.
[16] Schönheit, P., Moll, J. and Thauer, R.K. (1980) Arch. Microbiol. 127, 59–65.
[17] Bradford, M.M. (1976) Anal. Biochem. 72, 248–254.
[18] Johnson, M.K. (1988) in: Metal Clusters in Proteins (Que, L., Jr., Ed.), pp. 326–342. American Chemical Society, Washington, DC.
[19] Thomson, A.J., Cheesman, M.R. and George, S.J. (1993) Methods Enzymol. 226, 199–232.
[20] Johnson, M.K., Robinson, A.E. and Thomson, A.J. (1981) in: Iron-Sulfur Proteins (Spiro, T.G., Ed.), pp. 367–406, Wiley-Interscience, New York.
[21] Onate, Y.A., Finnegan, M.G., Hales, B.J. and Johnson, M.K. (1993) Biochim. Biophys. Acta 1164, 113–123.
[22] Brereton, P.S., Duderstadt, R.E., Staples, C.R., Johnson, M.K. and Adams, M.W.W.A. (1999) Biochemistry 38, 10594–10605.
[23] Thomson, A.J. and Johnson, M.K. (1980) Biochem. J. 191, 411–420.
[24] Bennett, D.E. and Johnson, M.K. (1987) Biochim. Biophys. Acta 911, 71–80.
[25] Johnson, M.K., Duderstadt, R.E. and Duin, E.C. (1999) Adv. Inorg. Chem. 47, 1–82.
[26] Johnson, M.K., Thomson, A.J., Robinson, A.E., Rao, K.K. and Hall, D.O. (1981) Biochim. Biophys. Acta 667, 433–451.
[27] Ciurli, S., Carrié, M., Weigel, J.A., Carney, M.J., Stack, T.D.P., Papaefthymiou, G.C. and Holm, R.H. (1990) J. Am. Chem. Soc. 112, 2654–2664.
[28] Middleton, P., Dickerson, D.P.E., Johnson, C.E. and Rush, J.D. (1980) Eur. J. Biochem. 104, 289–296.
[29] Noodleman, L. (1988) Inorg. Chem. 27, 3677–3679.
[30] Kappl, R., Ciurli, S., Luchinat, C. and Hütterman, J. (1999) J. Am. Chem. Soc. 121, 1925–1935.
[31] Schürmann, P., Stritt-Etter, A.-L. and Li, J. (1995) Photosynth. Res. 309, 309–312.
[32] Schürmann, P. and Gardet-Salvi, L. (1993) Chimia 47, 245–246.
[33] Glaser, T., Hedman, B., Hodgson, K.O. and Solomon, E.I. (2000) Acc. Chem. Res. 33, 859–868.
[34] Glaser, T., Rose, K., Shadle, S.E., Hedman, B., Hodgson, K.O. and Solomon, E.I. (2001) J. Am. Chem. Soc. 123, 442–454.
[35] Glaser, T., Bertini, I., Moura, J.J.G., Hedman, B., Hodgson, K.O. and Solomon, E.I. (2001) J. Am. Chem. Soc. 123, 4859–4860.